The Astrophysical Journal, 666:267–280, 2007 September 1

PROBING THE INTERSTELLAR MEDIUM NEAR STAR-FORMING REGIONS WITH GAMMA-RAY BURST AFTERGLOW SPECTROSCOPY: GAS, METALS, AND DUST

Jason X. Prochaska,[1] Hsiao-Wen Chen,[2] Miroslava Dessauges-Zavadsky,[3] and Joshua S. Bloom[4]

Received 2007 February 21; accepted 2007 May 15

ABSTRACT

We study the chemical abundances of the interstellar medium surrounding high-z gamma-ray bursts (GRBs) through analysis of the damped Lyα systems (DLAs) identified in afterglow spectra. These GRB DLAs are characterized by large H I column densities $N_{\rm H\,I}$ and metallicities [M/H] spanning 1/100 to nearly solar, with median $[{\rm M/H}] > -1$ dex. The majority of GRB DLAs have [M/H] values exceeding the cosmic mean metallicity of atomic gas at $z > 2$; i.e., if anything, the GRB DLAs are biased to larger metallicity. We also observe (1) large [Zn/Fe] values ($>+0.6$ dex) and subsolar Ti/Fe ratios, which imply substantial differential depletion; (2) large α/Fe ratios, suggesting nucleosynthetic enrichment by massive stars; and (3) low C^0/C^+ ratios ($<10^{-4}$). Quantitatively, the observed depletion levels and C^0/C^+ ratios of the gas are not characteristic of cold, dense H I clouds in the Galactic interstellar medium (ISM). We argue that the GRB DLA represents the ISM near the GRB but not gas directly local to the GRB (e.g., its molecular cloud or circumstellar material). We compare these observations with DLAs intervening in background quasars (QSO DLAs). The GRB DLAs exhibit larger $N_{\rm H\,I}$ values, higher α/Fe and Zn/Fe ratios, and higher metallicity than the QSO DLAs. Although these differences are statistically significant, the offsets are relatively modest ($N_{\rm H\,I}$ excepted). We argue that the differences result primarily from galactocentric radius-dependent differences in the ISM: GRB DLAs preferentially probe denser, more depleted, higher metallicity gas located in the inner few kiloparsecs, whereas QSO DLAs are more likely to intersect the less dense, less enriched, outer regions of the galaxy. Finally, we investigate whether dust obscuration may exclude GRB DLA sight lines from QSO DLA samples; we find that the majority of GRB DLAs would be recovered, which implies little observational bias against large $N_{\rm H\,I}$ systems.

Subject heading: quasars: absorption lines

Online material: color figures

1. INTRODUCTION

For the past decade, high-resolution spectroscopy of distant quasars (QSOs) has enabled detailed studies of the chemical abundances of high-z galaxies (e.g., Lu et al. 1996; Prochaska & Wolfe 1999; Dessauges-Zavadsky et al. 2001; Molaro et al. 2001; Prochaska et al. 2001; Ledoux et al. 2003). These properties of the ISM have been surveyed extensively via the DLAs, galaxies intersected by sight lines to distant quasars (for a review, see Wolfe et al. 2005). These QSO DLA sight lines sample galaxies according to gas cross section; i.e., the outer regions of a galaxy's ISM are more frequently probed because differential cross section is proportional to radius. If star formation (SF) occurs in compact regions in high-z galaxies (i.e., molecular clouds), then QSO DLAs would only rarely probe these environments (Zwaan & Prochaska 2006). This conclusion holds true independent of any additional biases related to dust obscuration by the SF regions themselves (e.g., Fall & Pei 1993). QSO DLA surveys are an inefficient approach to directly studying the gas in high-z SF regions.

Like quasars, GRBs provide a bright, albeit transient, light beam from the distant universe. Imprinted on the roughly power-law spectrum of the afterglow are the signatures of the intergalactic medium (e.g., Fiore et al. 2005; Chen et al. 2005; Prochter et al. 2006) and transitions from the ISM surrounding the GRB event (e.g., Savaglio et al. 2003; Vreeswijk et al. 2004; Prochaska et al. 2007a). And, analogous to absorption-line studies of quasars, these observations reveal the H I column density (Jensen et al. 2001; Vreeswijk et al. 2004; Jakobsson et al. 2006b), metallicity (Fynbo et al. 2006a; Prochaska 2006), chemical abundances, differential depletion (Savaglio & Fall 2004), and kinematics (Prochaska et al. 2007c) of the gas along the sight line.

The progenitors of long-duration GRBs are believed to be massive stars residing in active star-forming regions (Woosley 1993; Woosley & Bloom 2006). At low redshift, this association is well established: supernovae have been identified at the same position as GRB events (e.g., Hjorth et al. 2003; Stanek et al. 2003; Mirabal et al. 2006; see also Fynbo et al. 2006b). Furthermore, GRBs have been found recently to be located within Wolf-Rayet galaxies (Hammer et al. 2006). The connection between GRB and star-forming regions is inferred at high redshift. GRBs are found exclusively in galaxies that are blue and show nebular emission lines indicative of ongoing SF (e.g., Le Floc'h et al. 2003; Prochaska et al. 2004). Furthermore, high-precision astrometry of long-duration GRB afterglows reveals that these events occur exclusively within a few kiloparsecs of the flux-weighted centroid of their host galaxy (Bloom et al. 2002; Fruchter et al. 2006). Therefore, the sight lines to GRBs should probe the ISM within or at least near star-forming regions. In this respect, studies of the ISM along sight lines to GRBs complement those toward quasars.

The first observations of GRB DLAs indicated a large H I column density (Jensen et al. 2001; Vreeswijk et al. 2004) and large metal-line equivalent widths and column densities (Metzger et al.

[1] Department of Astronomy and Astrophysics, UCO/Lick Observatory, University of California, 1156 High Street, Santa Cruz, CA 95064; xavier@ucolick.org.

[2] Department of Astronomy, University of Chicago, 5640 South Ellis Avenue, Chicago, IL 60637; hchen@oddjob.uchicago.edu.

[3] Observatoire de Genève, 51 Chemin des Maillettes, 1290 Sauverny, Switzerland.

[4] Department of Astronomy, 601 Campbell Hall, University of California, Berkeley, CA 94720-3411.

1997; Savaglio et al. 2003). These data suggested modestly enriched gas ($\gtrsim$1/10 solar) and substantial depletion levels, but the analysis is limited by line saturation (i.e., low-resolution spectroscopy of lines with large optical depth; Prochaska 2006). With the launch of the *Swift* satellite (Gehrels 2000), GRBs are detected at a rate of $\approx$2 per week with rapid, precise localizations enabling echelle observations of a modest sample of GRB DLAs (Chen et al. 2005b; Prochaska et al. 2006, 2007a; Vreeswijk et al. 2007; Piranomonte et al. 2007). These observations provide precise column density measurements of many metal-line transitions and permit the analysis of the chemical abundances in the gas surrounding GRBs.

In this paper, we describe the chemical abundances of a modest sample of DLAs associated with the ISM surrounding GRBs. We focus on echelle observations acquired in the past 2 years, but also include pre-*Swift* observations. Our principal goal is to describe the physical conditions of the ISM within and/or near SF regions in the young universe. To frame the discussion, we compare the GRB DLA observations with similar sets of observations for DLAs along quasar sight lines (QSO DLAs).

There are at least three reasons why one may expect the ISM characteristics of the GRB DLAs to differ with those of QSO DLAs. First, the two samples may arise from overlapping yet nonidentical populations of high-z galaxies. By definition, the QSO DLAs correspond to galaxies with large H I surface densities. These are selected independently of any emission or stellar property (Wolfe et al. 1986), and cosmological simulations suggest that a subset may not even be located within dark matter halos (Razoumov et al. 2006). Long-duration GRBs, in contrast, are known to occur only within star-forming galaxies and are expected to roughly trace the ongoing SF rate (SFR; e.g., Wijers et al. 1998; Totani 1999; Ramirez-Ruiz et al. 2002; Guetta & Piran 2007). Of course, star-forming galaxies presumably also have large H I column densities,[5] as evidenced by the DLA profiles in GRB afterglows.

Second, even if QSO DLAs and GRB DLAs are drawn from the exact same parent population of host galaxies, the QSO DLAs are selected according to the H I covering fraction on the sky, while GRBs are expected to track the current SFR. One may expect QSO DLAs to preferentially arise in galaxies with extended H I disks (e.g., low surface brightness), whereas GRBs preferentially occur within high surface brightness galaxies (Mo et al. 1998). Finally, and perhaps most importantly, QSO DLAs will preferentially probe the outer regions of galaxies (Möller et al. 2002, 2004), whereas GRB DLAs are generally located within the inner few kiloparsecs of their host galaxies (Bloom et al. 2002; Fruchter et al. 2006). This could imply higher $N_{\rm H\,I}$ values, metallicity, depletion levels, molecular fractions, and differential rotation along the GRB DLA sight lines. Therefore, a secondary theme of this paper is to test the hypothesis that GRB DLAs and QSO DLAs are drawn from the same parent population of high-z galaxies and that any differences in ISM properties are explained by their average impact parameters through the galaxies.

This paper focuses primarily on results derived from spectroscopy of GRB optical afterglows. Additional constraints on the metal abundances and dust properties can be drawn from other observations (e.g., X-ray spectroscopy, afterglow photometry; Butler et al. 2006; Kann et al. 2006). We comment on these results when applicable and defer detailed comparisons to future analysis. This paper is organized as follows. Section 2 presents the experimental design, and observational samples. In § 3 we characterize the H I column densities, metallicities, relative abundances, and atomic carbon abundance of GRB DLAs. We discuss the implications of these results in § 4 and conclude with a list of future directions.

2. EXPERIMENTAL DESIGN AND OBSERVATIONAL SAMPLES

2.1. *Sight-Line Geometries*

Before discussing the observational data, it is important to comment further on a few fundamental differences between studying DLAs along GRB sight lines versus background QSOs. The most obvious differences are that the GRB sight line originates within the galaxy giving rise to the DLA and, almost certainly, from within a young star-forming region. This implies several important consequences for the DLAs probed by GRB afterglows.

First, because the phenomenon originates from within the DLAs themselves, a GRB sight line intersects less gas column than a background QSO sight line would at the same position on the sky. Therefore, one underestimates the average H I column density and may underestimate the total velocity field that occurs along the sight line. Second, it is possible that gas local to the progenitor, i.e., circumstellar material and/or molecular cloud gas, contributes significantly to the GRB DLAs (but see below). One may expect especially large dust-to-gas ratios, high molecular fractions, and/or peculiar chemical abundance ratios. Third, the GRB afterglow radiation can significantly affect the DLAs observed along its sight line, whereas QSO DLAs are selected to have a large distance from their background QSO. The UV flux from a GRB afterglow that is typical of high-resolution spectroscopic observations (i.e., peak magnitude of $R \approx 15$ at early times) is sufficient to ionize an H I column of approximately 10^{21} cm^{-2} at 5 pc from the afterglow in only a few minutes' time (e.g., Draine & Hao 2002; Perna & Lazzati 2002; Prochaska et al. 2006). Similarly, theoretical treatments predict that the X-ray and UV components of the afterglow can destroy dust and molecular hydrogen out to 10–100 pc (Waxman & Draine 2000; Fruchter et al. 2001; Draine & Hao 2002). If neutral gas and dust existed at distances of $\sim$10 pc prior to the burst, it is likely removed by the afterglow before spectroscopic observations are initiated. In this respect, the contribution of gas local to the GRB is somewhat minimized by the GRB event itself. By the same token, gas local to the star-forming regions may have been attenuated by the afterglow radiation field, and our observations may not precisely reflect the conditions of this gas in the absence of a GRB.

On the other hand, aside from the UV pumping of fine-structure lines (Prochaska et al. 2006; Dessauges-Zavadsky et al. 2006a; Vreeswijk et al. 2007), there is no compelling case of a GRB afterglow having attenuated its surrounding medium. There have been no substantiated reports of line variability in any resonance line, including—and most importantly—Mg I transitions. The majority of GRB DLAs exhibit strong Mg I absorption coincident in velocity with the resonance and excited transitions of low-ion species (Prochaska et al. 2006, 2007a). This atom has an ionization potential IP = 7.7 eV and would be ionized by the afterglow if it occurs within $\approx$100 pc of the event. Prochaska et al. (2006) have argued, therefore, that the majority of neutral gas observed in GRB DLAs is at a distance exceeding 100 pc from the progenitor. Meanwhile, the detection of UV-pumped excited states of Si^+, O^0, and Fe^+ requires that the gas is located within $\approx$1 kpc of the afterglow. Indeed, Vreeswijk et al. (2007) have analyzed variations in

[5] Similarly, we may expect that all galaxies with a large H I column density will exhibit SF. Indeed, the presence of heavy elements in all QSO DLAs indicates previous SF (Prochaska et al. 2003a), and C II* fine-structure absorption implies ongoing SF (Wolfe et al. 2003).

TABLE 1
GRB DLA Sample

GRB	R.A. (J2000.0)	Decl. (J2000.0)	z_{GRB}	Instrument	R	Mg I[a]	Exc. Fe II[b]	Ref.
GRB 990123.....	15 25 30.34	+44 45 59.1	1.600	Keck LRIS	1000	Y	N	1
GRB 000926.....	17 04 09.00	+51 47 10.0	2.038	Keck ESI	5000	Y	N	2, 3
GRB 010222.....	14 52 12.55	+43 01 06.2	1.477	Keck ESI	5000	Y	N	4
GRB 011211.....	11 15 17.98	−21 56 56.2	2.142	VLT FORS2	1000	?	N	1, 5
GRB 020813.....	19 46 41.87	−19 36 04.8	1.255	Keck LRIS	1000	Y	Y	6
GRB 030226.....	11 33 04.93	+25 53 55.3	1.987	Keck ESI	5000	?	N	7
GRB 030323.....	11 06 09.40	−21 46 13.2	3.372	VLT FORS2	1000	Y	N	8
GRB 050401.....	16 31 28.82	+02 11 14.8	2.899	VLT FORS2	1000	?	N	9
GRB 050505.....	09 27 03.20	+30 16 21.5	4.275	Keck LRIS	1000	?	N	10
GRB 050730.....	14 08 17.14	−03 46 17.8	3.969	Magellan MIKE	30,000	?	Y	11
GRB 050820.....	22 29 38.11	+19 33 37.1	2.615	Keck HIRES	30,000	N	N	12
GRB 050904.....	00 54 50.79	+14 05 09.4	6.296	Subaru FOCAS	1000	?	?	13
GRB 050922C	19 55 54.48	−08 45 27.5	2.199	VLT UVES	30,000	W	Y	14
GRB 051111	00 08 17.14	−00 46 17.8	1.549	Keck HIRES	30,000	Y	Y	12, 15
GRB 060206.....	13 31 43.42	+35 03 03.6	4.048	WHT ISIS	4000	?	?	16
GRB 060418.....	15 45 42.40	−03 38 22.80	1.490	Magellan MIKE	30,000	Y	Y	12

Note.—Units of right ascension are hours, minutes, and seconds, and units of declination are degrees, arcminutes, and arcseconds.
[a] Strong Mg I absorption (W = weak). GRB DLAs with strong Mg I absorption are likely to have the majority of their gas at distances greater than 50 pc from the afterglow (Prochaska et al. 2006).
[b] Positive detection of absorption from excited levels of Fe^+. This measurement is difficult in low-resolution data, and a nondetection should be interpreted as ambiguous. The absence of absorption in higher resolution data, however, indicates that the Fe^+ gas (observed via resonance lines) is at a large distance from the afterglow.
References.—(1) Savaglio et al. 2003; (2) Castro et al. 2003; (3) Fynbo et al. 2002; (4) Mirabal et al. 2002; (5) Vreeswijk et al. 2006; (6) Barth et al. 2003; (7) Shin et al. 2006; (8) Vreeswijk et al. 2004; (9) Watson et al. 2006; (10) Berger et al. 2006; (11) Chen et al. 2005b; (12) Prochaska et al. 2007a; (13) Kawai et al. 2006; (14) Piranomonte et al. 2007; (15) Prochaska et al. 2006; (16) Fynbo et al. 2006a.

the level populations of the excited levels of Fe^+ and Ni^+ and constrain the distance of the GRB DLAs along the GRB 060418 sight line to be at 1 ± 0.2 kpc from the afterglow.

Table 1 indicates those GRB DLAs that exhibit strong Mg I absorption. We also identify the GRB DLAs that show absorption from excited states of Fe^+. Those cases without Fe^+ fine-structure absorption must also lie at distances $\gtrsim$100 pc (Prochaska et al. 2006; Chen et al. 2007). These results indicate that the majority of gas in GRB DLAs is not local to the SF region and should not be adversely affected by the GRB afterglow. It is possible, of course, that some components of the absorption-line profiles (i.e., any that are absent Mg I and fine-structure absorption) lie at distances less than 100 pc. Similarly, there is frequently high-ion absorption (i.e., C IV; Chen et al. 2007) that is not coincident with Mg I or fine-structure absorption. We emphasize, however, that the fine-structure and Mg I profiles are generally aligned with the peak in the optical depth of the low-ion resonance lines (Prochaska et al. 2007c). Therefore, it is reasonable to place the "clouds" that dominate the metal abundances of the gas at distances $\gtrsim$100 pc.

Our current expectation is that O and B stars from the star-forming region have ionized all gas within $\approx$100 pc of the GRB producing large H II regions. Figure 1 presents a cartoon illustration of a GRB and a QSO sight line through a galaxy comprised of a neutral ISM surrounded by predominantly ionized halo gas clouds. The GRB sight line originates near the center of the galaxy, within an H II region associated with ongoing star formation. In contrast, the QSO DLA sight lines will preferentially penetrate the outer regions of the ISM.

Independent of the differences one may expect for QSO DLAs and GRB DLAs, there may be common trends (e.g., metallicity vs. dust depletion) characteristic of the ISM of all high-z galaxies. By considering the QSO DLAs and GRB DLAs together, we hope to reveal these global trends, in addition to highlighting differences in the samples.

2.2. *GRB DLA and QSO DLA Samples*

The QSO DLA samples are drawn from two sources: (1) high-resolution echelle and echellette observations of quasars acquired with the High Resolution Echelle Spectrometer (HIRES; Vogt et al. 1994) and Echelette Spectrograph and Imager (ESI; Sheinis et al. 2000) at the Keck Observatory, and the UV-Visual Echelle Spectrograph (UVES; Dekker et al. 2000) at the Very Large Telescope (VLT) observatory; and (2) the low-resolution QSO DLA surveys of the Sloan Digital Sky Survey (SDSS; Prochaska & Herbert-Fort 2004; Prochaska et al. 2005). We restrict the samples

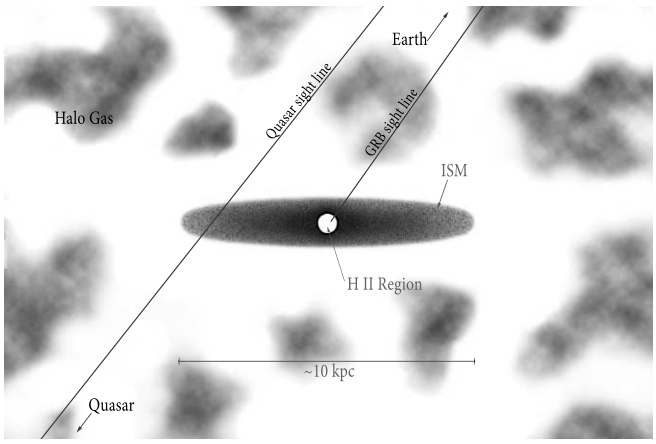

Fig. 1.—Cartoon illustrating the likely differences between QSO DLA and GRB DLA sight lines. The former have randomly intersected a foreground galaxy. These QSO DLA sight lines correspond to a cross-section-selected sample and should preferentially intersect the outer regions of the ISM in high-z galaxies. In contrast, the GRB DLAs are constrained to originate from within the ISM of their host galaxies, presumably the H II region produced by massive stars in a star-forming region. These GRB DLA sight lines are expected (and observed) to originate within the inner few kiloparsecs of the ISM.

TABLE 2
QSO DLA Samples

Sample	Description	$N_{\rm DLA}$	Instrument(s)	Reference
HR-A	High-resolution full sample (all)	153	HIRES, ESI, UVES	1, 2, 3, 4, 5
HR-S	High-resolution "statistical" sample	112	HIRES, ESI, UVES	5
HR-E	High-precision echelle	71	HIRES, UVES	1, 2
SDSS	True ($N_{\rm H\,I}$) statistical sample	475	SDSS	6, 7

References.—(1) Prochaska et al. 2007b; (2) Dessauges-Zavadsky et al. 2006b; (3) Ledoux et al. 2006; (4) Herbert-Fort et al. 2006; (5) Prochaska et al. 2003a; (6) Prochaska & Herbert-Fort 2004; (7) Prochaska et al. 2005.

to $z_{\rm DLA} > 1.6$ and DLAs that are greater than 3000 km s^{-1} from their background quasar. The high-resolution sample (HR-A) is summarized in Herbert-Fort et al. (2006), Ledoux et al. (2006), Dessauges-Zavadsky et al. (2006b), and Prochaska et al. (2007b). Prochaska et al. (2007b) have emphasized that the full data set is a heterogeneous sample of QSO DLAs, including a number of systems selected on the basis of strong metal lines (Herbert-Fort et al. 2006) or as promising candidates for H_2 absorption (Ledoux et al. 2003). As such, the H I distribution $f(N_{\rm H\,I})$ of the high-resolution sample does not follow the statistical distribution derived from the SDSS.

For a number of the comparisons made in this paper, we take subsets of these samples. In particular, we define a pseudostatistical sample of metallicity measurements (HR-S) that is restricted to the compilation of Prochaska et al. (2003a). We also construct a sample of high-quality echelle-only observations (HR-E) for analysis related to relative abundances (e.g., α/Fe). The echellette observations, in particular, have too poor data quality to generally achieve better than 0.1 dex precision (Prochaska et al. 2003b) and are not included. Although the DLAs in these high-resolution subsets do not follow $f(N_{\rm H\,I})$ for a random sample, they were selected only on the basis of a large H I column density. Table 2 summarizes the various QSO DLA samples considered in this paper.

Our selection criteria for the GRB DLA sample are (1) the presence of a DLA ($N_{\rm H\,I} \geq 2 \times 10^{20}$ cm^{-2}) or a low-ion column density that requires $N_{\rm H\,I}$ to exceed 2×10^{20} cm^{-2}, assuming solar metallicity;[6] and (2) spectra with a sufficient signal-to-noise ratio (S/N) and resolution to study the chemical abundances of the gas. The sample is also limited to GRB DLAs for which we could access the data or for which precise equivalent width measurements were reported in the literature. Table 1 lists the GRB DLAs comprising our sample and describes the spectral observations.

As with QSO DLAs (Fall & Pei 1993), it is likely that dust obscuration plays a role in defining the GRB DLA sample. There are several examples in the literature of highly reddened afterglows that are likely extinguished by dust in the GRB host galaxy (e.g., Levan et al. 2006; Pellizza et al. 2006). At present, no comprehensive study on the incidence of optically "dark" bursts has been performed, nor an evaluation of the fraction of dark bursts that are cases of dust obscuration (as opposed to high-z events). We expect, however, that dust obscuration is important to defining GRB DLA samples.

2.3. *Absorption-Line Metallicities*

Metallicity is the mass density in metals relative to hydrogen and helium gas. It is likely that oxygen dominates this quantity in nearly every astrophysical environment, with carbon and nitrogen being secondary. Although these three elements exhibit low-ion transitions, the majority are either too strong, too weak, and/or located within the Lyα forest. Therefore, the metal abundance of the ISM is frequently gauged by other elements. Unfortunately, many of the transitions that are accessible to analysis arise from elements that are refractory (Pettini et al. 1990). To avoid the complications of depletion corrections (which can be an order of magnitude or more), observers have focused on nonrefractory or mildly refractory elements. These include S, Si, and Zn. The latter is a trace element, $\log ({\rm Zn/H})_\odot = -7.3$, with an uncertain nucleosynthetic origin (Hoffman et al. 1996), and therefore should be considered cautiously.

A point of great interest in GRB studies is the metallicity of the progenitor, especially in the context of the collapsar model (Woosley 1993). In the collapsar paradigm, large angular momentum is required to power the GRB. Because high-metallicity stars are expected to have significant mass loss by winds promoting the loss of angular momentum (Vink & de Koter 2005), Langer & Norman (2006) and Woosley & Heger (2006) have argued that GRB progenitors will have low metallicity, i.e., less than 1/10 solar abundance. One may consider this to be a natural prediction of the collapsar model.

There is at least circumstantial evidence in support of a metallicity "bias" from studies of $z < 1$ GRB host galaxies. The metallicities of the H II regions in a small sample of $z < 0.5$ galaxies hosting GRBs are subsolar (Prochaska et al. 2004; Sollerman et al. 2005), and several authors have noted that the values are systematically lower than the predicted distribution for galaxies drawn randomly according to the current SFR (Stanek et al. 2006; Kewley et al. 2007; Modjaz et al. 2007). Furthermore, the GRB host galaxies at $z \sim 1$ are generally sub-L_*, consistent with low metallicity (Le Floc'h et al. 2003). Fruchter et al. (2006) compared a sample of $z \lesssim 1$ GRB host galaxies against the host population for core-collapse supernovae and demonstrated that GRB host galaxies have systematically lower luminosities. The difference is approximately 1 mag, which they suggested could be due to a metallicity bias. However, galaxies follow a metallicity-luminosity relation that is roughly linear (Kobulnicky & Kewley 2004), and a 1 mag difference in luminosity implies only an approximately 0.3 dex offset in metallicity. Recently, Wolf & Podsiadlowski (2007) performed a thorough analysis, showing that the observations suggest a metallicity "ceiling" for GRB progenitors but that this cutoff occurs at no lower than 1/2 solar. Therefore, while the offset in luminosities between the host galaxies of GRBs and core-collapse supernovae may be explained by a metallicity bias, this does not imply as severe an effect as that promoted by studies of mass loss.

At high redshift, it is difficult to observe nebular lines to measure metallicities, and our knowledge of galaxies is too poor to make robust statements from luminosity distributions alone. Instead, one can measure the metallicity of the ISM from

[6] We note that the few GRB sight lines with $N_{\rm H\,I} < 10^{20}$ cm^{-2} have very low column densities for low-ion transitions (Fiore et al. 2005; Prochaska et al. 2005).

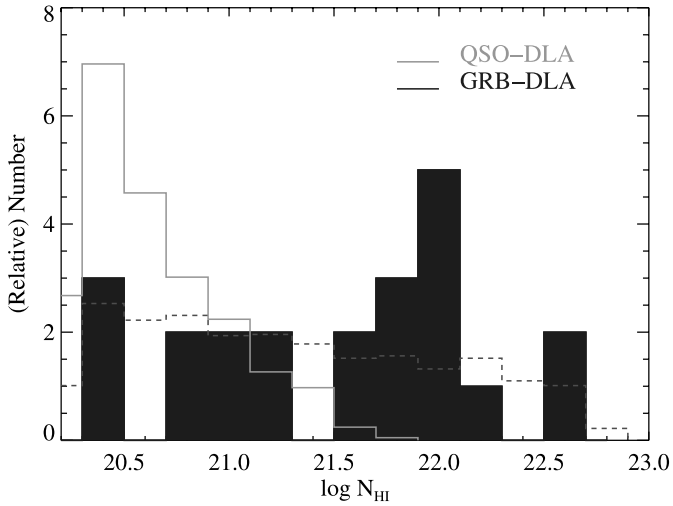

FIG. 2.—*Solid curve*: Traces the histogram of $N_{\rm H\,I}$ values for the GRB DLAs. In comparison, we show a histogram of $N_{\rm H\,I}$ values for QSO DLAs drawn randomly toward background quasars (Prochaska et al. 2005) and normalized for presentation to have the same number of systems as the GRB DLA sample. The GRB DLAs have a median value $\log N_{\rm H\,I} = 21.7$, which exceeds all but a few QSO DLAs observed to date. *Dashed line*: Traces the predicted distribution of $N_{\rm H\,I}$ values, assuming a sample of sight lines originating inside an H II region located at the center of an H I exponential disk. The model shown has central column density $\log N_0 = 22$, scale height to scale radius $h/R = 0.1$, and an H II region with radius $r_{\rm H\,II} = 4h$. [*See the electronic edition of the Journal for a color version of this figure.*]

absorption-line spectroscopy by comparing the total hydrogen column density with the total column density of metals.

3. GAS-PHASE ABUNDANCES IN GRB DLAs

In this section, we present column densities of hydrogen and metals observed in the gas phase in GRB DLAs. These observations give the surface density and metallicity of the ISM, and the relative abundances reflect differential depletion and the underlying nucleosynthetic patterns in the gas. Finally, we comment on the abundance of atomic carbon. In all of this analysis, we draw comparisons between the GRB DLAs and QSO DLAs.

3.1. *Hydrogen Column Densities*

In principle, the absorption-line spectra of rest-frame UV transitions ($\lambda < 3000$ Å) will give measurements of the atomic hydrogen and molecular hydrogen column densities, $N_{\rm H\,I}$ and $N_{\rm H_2}$. For a DLA, the former is best determined through a Voigt profile fit to the Lyα λ1215 transition. At $N_{\rm H\,I} > 10^{20}$ cm^{-2}, the damping wings of the Lorentzian line profile are well resolved with a moderate-resolution spectrum (FWHM < 5 Å). Therefore, aside from the redshift, the $N_{\rm H\,I}$ value is the most readily measured physical characteristic of a DLA.

Figure 2 presents the sample of $N_{\rm H\,I}$ measurements for our GRB DLA sample, supplemented by the compilation of Jakobsson et al. (2006a) and compared against the distribution of $N_{\rm H\,I}$ values for QSO DLAs measured from the SDSS (Prochaska et al. 2005). As previously reported (Vreeswijk et al. 2004; Jakobsson et al. 2006a), the GRB DLA distribution is skewed to significantly higher $N_{\rm H\,I}$ values than QSO DLAs. The difference, at least qualitatively, supports the hypothesis that QSO DLAs probe the outer regions of galaxies, whereas GRB DLAs probe the inner, star-forming regions. Jakobsson et al. (2006a) discussed that the GRB DLA distribution is roughly consistent with that predicted for GRBs embedded within molecular clouds (Reichart & Price 2002). The authors note, however, that GRBs exhibit too many sight lines with $N_{\rm H\,I} < 10^{22}$ cm^{-2} compared to the prediction for molecular clouds. They argue that this may result from photoionization and/or because GRBs are preferentially located at the edge (White et al. 1999) or even outside molecular clouds (Hammer et al. 2006).

As we discussed in § 2.1, however, the presence of strong Mg I absorption in nearly every GRB sight line argues that the majority of GRB DLA gas is located beyond ≈100 pc of the event. This distance is comparable to only the largest giant molecular cloud complexes in the Local Group (Blitz et al. 2007), and it is reasonable to assume that the GRB DLA gas is generally not associated with the molecular cloud hosting the GRB (see § 4.1). Examining Figure 2 in this light, the most salient question becomes: why do GRB DLAs exhibit a preponderance of $N_{\rm H\,I} > 10^{22}$ cm^{-2} measurements? Indeed, the gas mass required to average $N_{\rm H\,I} = 10^{22}$ cm^{-2} at 100 pc along random sight lines is $M_{\rm H\,I} = 10^7\ M_\odot$; this exceeds the masses of even the largest molecular clouds in the Milky Way (Solomon & Rivolo 1989; Blitz 1993). It seems unlikely, therefore, that the observed H I gas corresponds to the circumstellar medium that hosted the GRB. Instead, we contend that the gas is associated with the nearby ISM of the galaxy. This hypothesis, however, must account for the large $N_{\rm H\,I}$ values while allowing for an evacuated volume (i.e., H II region) with a radius of 100 pc or more.

To explore this point further, we considered an H I disk described by a double exponential,[7]

$$n(Z,R) = \frac{N_0}{h}\exp\left(\frac{-|Z|}{h}\right)\exp\left(\frac{-R}{R_d}\right), \qquad (1)$$

with scale height h, disk length R_d, and central H I column density N_0. We searched a wide parameter space of h/R_d, N_0, and radius of the H II region $r_{\rm H\,II}$. Overplotted on Figure 2 is the prediction for random sight lines originating at the center and midplane ($R = Z = 0$) of an exponential disk with $\log N_0 = 22$, $h/R_d = 0.1$, and $r_{\rm H\,II} = 4h$. This is a reasonably good description of the observed distribution ($P_{\rm KS} = 11\%$); an ambient ISM characterized by $\log N_0 = 22$ with a large H II region ($r_{\rm H\,II} > 2h$) produces a reasonable model for the observed $N_{\rm H\,I}$ distribution. It would be worthwhile to consider this model within the context of star-forming galaxies in cosmological simulations.

The association of GRBs with star-forming regions raises the possibility that a significant fraction of the gas in GRB DLAs is molecular. Conveniently, H_2 gives rise to several band heads at $\lambda \approx 1000$ Å, and one can directly measure the H_2 column density. For optical spectroscopy, this requires $z_{\rm GRB} > 2$ and blue wavelength coverage. It is also important to have relatively high resolution to disentangle the absorption lines from the Lyα forest. Tumlinson et al. (2007) have recently presented an analysis of five GRB sight lines and set an upper limit to the molecular fraction $f(H_2) < 10^{-5}$ in four of the systems. The only tentative detection is along the sight line to GRB 060206, with $f(H_2) \approx 10^{-3.5}$ (Fynbo et al. 2006a), and even this value is likely to be an upper limit (Tumlinson et al. 2007). Therefore, we assume that $N_{\rm H_2}$ is a small fraction of the total hydrogen column density. These results lend further support to the interpretation of GRB DLAs as being dominated by ambient ISM instead of gas local to the progenitor.

Finally, there is the contribution to N(H) from H^+. Out to distances of several tens of pc, the SF region (or GRB afterglow) will have produced an H II region with a potentially large $N_{\rm H\,I}$

[7] The following results are not too sensitive to the functional form of the radial profile.

TABLE 3
GRB DLA Abundance Summary

GRB	log $N_{\rm H\,I}$	f_α[a]	[α/H]	$\sigma(\alpha)$[b]	$f_{\rm Zn}$[c]	[Zn/H]	σ(Zn)[b]	$f_{\rm M}$[d]	[M/H]	σ(M)[b]	$f_{\rm Fe}$[e]	[Fe/H]	σ(Fe)[b]	[Ti/H][f]	$f_{\rm N}$[c]	[N/H]	σ(N)	$N(C^0)$[g]
GRB 990123.....	22[h]	0	...	...	2	−0.97	LL	12	−0.97	LL	2	−2.00	LL	...	0	...	...	...
GRB 000926.....	$21.30^{+0.25}_{-0.25}$	2	−1.58	LL	1	−0.17	0.15	2	−0.17	0.29	5	−1.49	0.08	−0.43	0	...	...	13.9
GRB 010222.....	22[h]	2	−1.61	LL	2	−1.30	LL	12	−1.30	LL	1	−2.01	0.08	−2.35	0	...	...	...
GRB 011211	$20.40^{+0.20}_{-0.20}$	2	−1.36	LL	0	...	...	11	−1.36	LL	2	−1.80	LL	...	0	...	...	...
GRB 020813.....	22[h]	2	−1.31	LL	2	−1.17	LL	12	−1.17	LL	2	−2.10	LL	−1.94	0	...	...	...
GRB 030226.....	$20.50^{+0.30}_{-0.30}$	2	−1.31	LL	3	−0.47	UL	11	−1.31	LL	1	−1.05	0.18	...	0	...	...	...
GRB 030323.....	$21.90^{+0.07}_{-0.07}$	2	−1.56	LL	2	−0.87	LL	12	−0.87	LL	1	−2.40	0.43	...	0	...	...	...
GRB 050401.....	$22.60^{+0.30}_{-0.30}$	2	−2.16	LL	2	−1.57	LL	12	−1.57	LL	2	−2.30	LL	...	0	...	...	...
GRB 050505.....	$22.05^{+0.10}_{-0.10}$	−4	−1.25	LL	0	...	...	11	−1.25	LL	2	−1.35	LL	...	0	...	...	...
GRB 050730.....	$22.15^{+0.10}_{-0.10}$	4	−2.26	0.10	0	...	...	4	−2.26	0.14	1	−2.50	0.08	...	1	−3.16	0.10	13.2
GRB 050820.....	$21.00^{+0.10}_{-0.10}$	4	−0.63	0.04	1	−0.71	0.02	4	−0.63	0.11	1	−1.60	0.09	−0.80	2	−1.35	LL	12.7
GRB 050904.....	$21.30^{+0.20}_{-0.20}$	−4	−1.10	LL	0	...	...	11	−1.10	LL	0	...	...	...	0	...	...	...
GRB 050922C.....	$21.60^{+0.10}_{-0.10}$	4	−2.03	0.10	3	−2.02	UL	4	−2.03	0.14	1	−2.63	0.01	−1.60	3	−4.09	UL	12.9
GRB 051111	22[h]	2	−1.42	LL	2	−0.96	LL	12	−0.96	LL	1	−2.14	0.01	−2.23	0	...	...	13.0
GRB 060206.....	$20.85^{+0.10}_{-0.10}$	4	−0.85	0.15	0	...	...	4	−0.85	0.18	0	...	...	...	0	...	...	...
GRB 060418.....	22[h]	2	−1.67	LL	1	−1.65	0.04	2	−1.65	1.00	1	−2.24	0.03	−2.23	0	...	...	12.9

Note.—With the exception of [M/H], the errors reported in the [X/H] values only reflect uncertainty in X.
[a] 0 = No measurement; 1 = Si measurement; 2 = Si lower limit; 3 = Si upper limit; 4 = [S/H]; 5 = [O/H]; 13 = S+Si limits; −4 = S lower limit.
[b] UL indicates upper limit; LL indicates lower limit.
[c] 0 = No measurement; 1 = Measurement; 2 = Lower limit; 3 = Upper limit.
[d] 0 = No measurement; 1 = Si measurement; 2 = Zn measurement; 3 = Combination of limits; 4 = S measurement; 11 = Lower limit from [α/H]; 12 = Lower limit from Zn.
[e] 0 = No measurement; 1 = Fe measurement; 2 = Fe lower limit; 3 = Fe upper limit; 4 = [Ni/H] − 0.1 dex; 5 = [Cr/H] − 0.2 dex.
[f] Upper limit on the Ti abundance.
[g] Upper limit on the column density of atomic carbon.
[h] Because $z_{\rm GRB} < 1.6$, Lyα was not observed. We have set $N_{\rm H\,I} = 10^{22}$ cm^{-2}, the median value of GRB DLAs.

value—that is, unless stellar winds from the GRB progenitor have nearly evacuated the region altogether. There is, of course, no direct means of measuring the H^+ column density. Instead, we restrict our analysis of the metal column density to the atoms and ions that are dominant in neutral regions. These are termed "low ions": Si^+, Fe^+, C^+, and O^0. We caution that low ions are not entirely absent from H II regions (e.g., Howk & Sembach 1999), although the expected contribution would be small compared to neutral gas for $N_{\rm H\,I} > 10^{21}$ cm^{-2}. A detailed treatment of the ionization state of GRB DLAs will be presented in a future paper. Here, we assume that ionization corrections are small and comment on conclusions that are sensitive to this assumption.

3.2. *GRB DLA Metallicities*

Ideally, the metal column density is derived from a single or set of unsaturated, resolved transitions of a low ion. We do not attempt to measure the total column density of each element (i.e., by summing all of the ionization states of a given element); rather, we measure only the state that is dominant in neutral hydrogen regions (the low ion). This can generally be achieved from spectra with high-resolution observations and a modest S/N. To date, however, many GRB spectra have been acquired with low-resolution spectrometers. These observations may provide accurate measurements of the equivalent widths (EWs) of strong lines, but precise column densities are difficult to derive due to modeling the line profile (Jenkins 1986). The high-resolution observations of GRB DLAs, however, indicate that the metal-line profiles are comprised of multiple components (termed "clouds") that exhibit a bimodal or even more complicated distribution of column densities (Prochaska 2006). In most cases, the total column density is dominated by a single or few clouds, whereas the EW is the net sum of many weak clouds. When the cloud column densities exhibit a bimodal distribution, the single-component curve-of-growth (COG) analysis systematically underestimates the ionic column densities (Jenkins 1986; Prochaska 2006). In the following, we use low-resolution EW observations only to set lower limits to column density measurements and exclude these from relative chemical abundances.

Table 3 summarizes the abundance measurements for the GRB DLAs. We have corrected ions that exhibit fine-structure splitting of the ground state (e.g., Fe^+) by the observed contribution of these levels. In general, this implies an increment of <0.05 dex. In five cases the H I column density and a nonrefractory or mildly refractory metal abundance have been precisely measured. For the remainder of cases, we report a lower limit to the metallicity because the metal abundance is a lower limit and/or there is no spectral coverage of the Lyα transition. In the latter cases, we have assumed $N_{\rm H\,I} = 10^{22}$ cm^{-2}, which is approximately the mean log $N_{\rm H\,I}$ value of GRB DLAs.

We have evaluated the metallicity of the gas by adopting (in order of preference) the [S/H] value,[8] [Si/H] value, [Zn/H] value, or the maximum of these if each has only a lower limit value. We prefer S and Si to Zn because these elements are $\approx$1000 times more abundant and because Zn has an uncertain nucleosynthetic origin (Hoffman et al. 1996). Again, we avoid highly refractory elements such as Fe and Ni (although they may dominate the opacity in stellar atmospheres and therefore are particularly relevant within the collapsar model) because these elements may be depleted from the gas phase.

Figure 3 presents the metallicity measurements for the GRB DLAs as a function of the age of the universe (set by $z_{\rm GRB}$) assuming the concordance cosmology ($\Omega_\Lambda = 0.72$, $\Omega_m = 0.28$, $h = 0.73$; Spergel et al. 2007). Overplotted on the figure are the metallicity measurements for the statistical sample (HR-S) of QSO DLAs. We restrict the discussion in this section to $t < 3.5$ Gyr (i.e., $z > 1.65$), at which all of the GRB DLAs have measured $N_{\rm H\,I}$ values. It is apparent that both the GRB DLAs and QSO DLAs exhibit a large dispersion of values. The peak-to-peak range is

[8] $[X/Y] = \log(X/Y) - \log(X/Y)_\odot$.

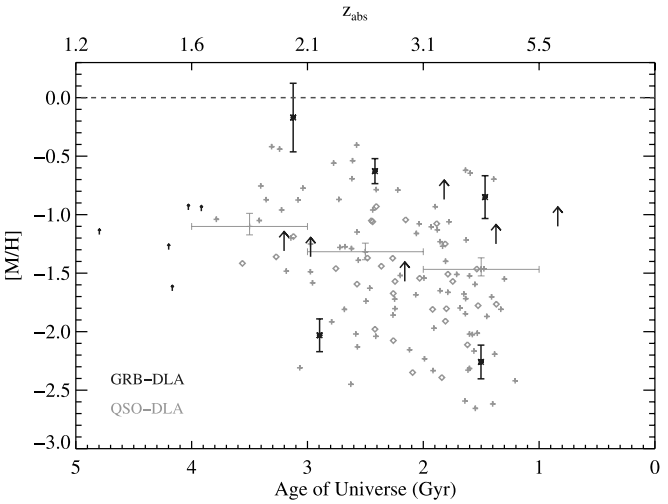

FIG. 3.—Metallicity [M/H] measurements for the GRB DLAs (*black*) as a function of the age of the universe, corresponding to the observed absorption redshift and assuming the current concordance cosmology (Spergel et al. 2007). At $z < 1.6$, where Lyα is lost below the atmosphere, the small arrows indicate lower limits to the metallicity, assuming $N_{\rm H\,I} = 10^{22}$ cm^{-2}. At $z > 1.6$, the lower limits to [M/H] for the GRB DLAs are due to line saturation. The lighter points show measurements for the QSO DLAs, assuming the HR-S sample (Prochaska et al. 2003a). The plus signs indicate $N_{\rm H\,I} < 10^{21}$ cm^{-2}, and the diamonds correspond to $N_{\rm H\,I} \geq 10^{21}$ cm^{-2}. We also present the cosmic mean metallicity derived from the QSO DLAs by taking the H I–weighted mean of the individual data points. Comparing the two distributions, we note that the majority of GRB DLA values lie above the cosmic mean and that a significant fraction have [M/H] > -1. [*See the electronic edition of the Journal for a color version of this figure.*]

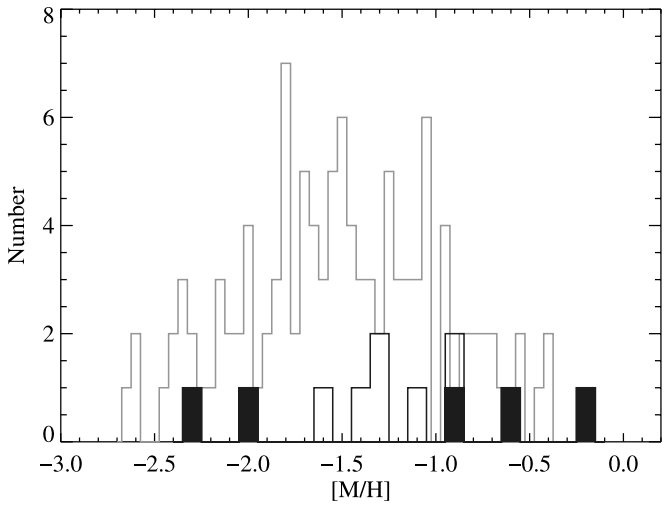

FIG. 4.—Histogram of [M/H] measurements for the QSO DLAs (*gray*) and the GRB DLAs (*black*), with both samples restricted to $z > 1.6$. For the GRB DLAs, the open histogram traces the lower limits to [M/H] because of line saturation. If these values are evaluated as measurements, then the two distributions are consistent with being drawn from the same parent population. If we increment the lower limits by +0.3 dex, however, the null hypothesis is ruled out at >99% c.l. by a two-sided KS test. Similarly, a two-sample survival analysis (Feigelson & Nelson 1985) rules out the null hypothesis at greater than 99% c.l. [*See the electronic edition of the Journal for a color version of this figure.*]

≈2 dex, much larger than observational uncertainty. Second, both samples exhibit a metallicity "floor" at approximately 1/1000 solar abundance. This lower limit to the metallicities is also not observational; the sensitivity limit of the data is at least an order of magnitude lower. It remains an open question whether this floor is associated with early (Population III) enrichment or rapid local enrichment in all galaxies exhibiting DLAs (Wasserburg & Qian 2000; Prochaska et al. 2003a; Qian & Wasserburg 2003).

Also overplotted in Figure 3 is the cosmic mean metallicity of atomic gas. This quantity is derived from the $N_{\rm H\,I}$-weighted mean of QSO DLA metallicities (Lanzetta 1993; Prochaska et al. 2003a). Six of the 10 GRB DLAs with $N_{\rm H\,I}$ measurements exceed the cosmic mean, and several lower limits lie at the cosmic mean. Therefore, many and likely most of the GRB DLAs have metallicities exceeding the cosmic mean in the ambient ISM of high-z galaxies. On these grounds, at least, the GRB DLAs at high z do not appear to show a significant metallicity bias toward low values (see also Fynbo et al. 2006a).

Figure 4 presents a histogram of [M/H] values for the GRB DLAs and QSO DLAs (restricted to $z > 1.6$). The filled bars indicate GRB DLA values while the dark open bars show lower limits to [M/H] for the GRB DLAs. We observe that the GRB DLA values roughly overlap the QSO DLA distribution. A proper treatment of the observations is to perform a two-sample survival analysis (Feigelson & Nelson 1985). Using the ASURV software package, we ran standard Gehan, logrank, and Peto-Peto tests using the Kaplan-Meier estimator and found that the null hypothesis is ruled out at 99% c.l. We conclude that the metallicities of GRB DLAs are larger than those for QSO DLAs at $z > 1.6$.

We note that many of the GRB DLAs have a metallicity greater than 1/10 solar. At first glance, this appears to contradict assertions that GRB progenitors have metallicity less than 0.1 $Z_\odot$ (Langer & Norman 2006; Woosley & Heger 2006). We demonstrate in § 3.3, however, that the gas-phase abundances of S, Si, and Zn are all enhanced relative to Fe. The data allow, but do not require, that the abundance of Fe is ≈0.5 dex lower than the [M/H] values. It is possible, therefore, that at high z the GRB DLA metallicities are not biased low and also that [Fe/H] < -1 in most cases. And, if Fe dominates the opacity in the atmospheres of massive stars (e.g., Vink & de Koter 2005), this is the most relevant quantity to consider. Finally, the gas that we observe is many tens of pc away from the progenitor and need not accurately reflect its metallicity. On the other hand, the GRB progenitor is expected to be a young, massive star, and its metallicity should not be too different from its host galaxy. At present, therefore, we have no reason to suspect that the ISM values would systematically overestimate the GRB progenitor metallicity.

3.3. *Relative Abundances*

We now turn our attention to the relative abundances of the GRB DLAs. These are measured by comparing the gas-phase column densities of pairs of low ions (X_i, Y_i) under the assumption that ionization corrections are small; i.e., $[X/Y] = \log N_{X_i} - \log N_{Y_i} - \log (X/Y)_\odot$. With high-resolution observations and moderate-S/N data, one can frequently achieve 0.05 dex precision or better for $\log N_{X_i}$. Because the observed ratios represent gas-phase abundances, however, the values reflect a combination of the underlying nucleosynthetic pattern and the effects of differential depletion onto dust grains. It is unfortunate that there is no element in the Fe peak that is nonrefractory. As such, observers frequently employ Zn (a neighbor of the Fe peak) as a surrogate for Fe because it is nonrefractory and because it traces Fe in the Galaxy at [Fe/H] > -2 (Sneden et al. 1991). We note, however, that Zn has an uncertain nucleosynthetic origin and should not directly trace Fe in galaxies whose SF history differs from that of the Milky Way (Fenner et al. 2004). Therefore, we consider it to be a surrogate for Fe but with a large systematic uncertainty.

Throughout this section we restrict the QSO DLA sample to the high-precision echelle measurements (sample HR-E; Table 1).

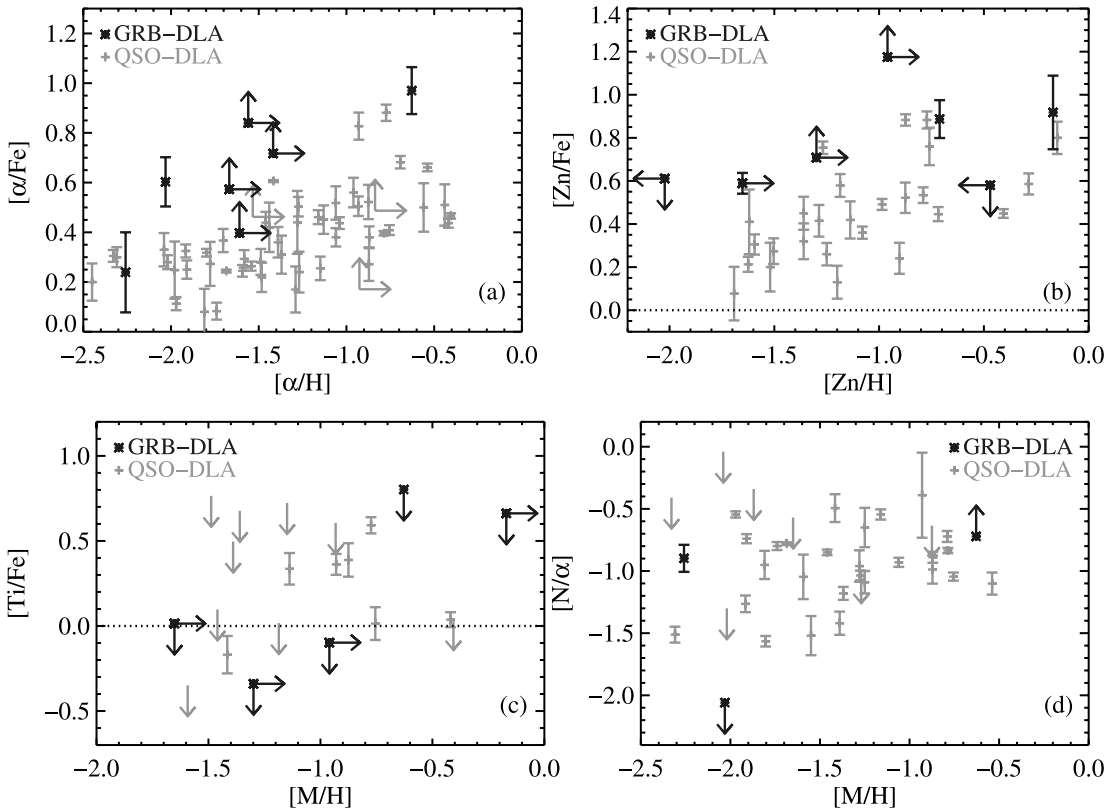

FIG. 5.— Observed gas-phase relative abundances as a function of alpha abundance [α/H], zinc abundance [Zn/H], or metallicity [M/H]. The four panels show the values for GRB DLAs and QSO DLAs (sample HR-E) for (*a*) [α/Fe] ratios, (*b*) [Zn/Fe] ratios, (*c*) [Ti/Fe] ratios, and (*d*) [N/α] ratios. The GRB DLAs are characterized by large [α/Fe] and [Zn/Fe] ratios, indicating significant nucleosynthetic enhancement by massive stars and/or differential depletion. One also notes several solar and subsolar upper limits on [Ti/Fe], which are strong evidence that refractory metals are depleted onto dust grains in GRB DLAs. [*See the electronic edition of the Journal for a color version of this figure.*]

3.3.1. α/Fe

A key nucleosynthetic diagnostic of stars and galaxies is the α/Fe ratio, where α refers to the sequence of He fusion in massive stars, i.e., O, Mg, Si, S, and Ar. The standard theory of nucleosynthesis predicts that these elements are predominantly produced by massive stars (e.g., Woosley & Weaver 1995). Therefore, a comparison of the α-abundance with the Fe-peak observations, whose production is dominated by the Type Ia supernovae (SNe) of less massive stars, constrains the age and SF history of the galaxy when plotted against gas metallicity (Tinsley 1979). Unfortunately, O and Mg are difficult to measure via UV absorption lines because the transitions are either too strong or too weak. Instead, one typically estimates the α-abundance with Si or S. In the QSO DLAs, [S/Si] $\approx$ 0, and the elements are roughly interchangeable (Prochaska & Wolfe 2002). For the GRB DLAs, we have also adopted these two elements as the reference for α. The Fe-peak abundance, meanwhile, is determined from Fe, Ni, or Cr.

Figure 5*a* presents the observed α/Fe ratios for the GRB DLAs against the QSO DLAs as a function of α-abundance, [α/H]. We reemphasize that these gas-phase abundances have not been corrected for differential depletion. Consider, first, the values for the QSO DLAs. At low metallicity ([α/H] < -1.5), the QSO DLAs follow a well-defined "plateau" at [α/Fe] $\approx$ 0.25 dex (Prochaska & Wolfe 2002). This plateau matches the one observed for metal-poor Galactic stars (McWilliam 1997), suggesting that the α/Fe enhancement has a nucleosynthetic origin (Lu et al. 1996; Dessauges-Zavadsky et al. 2006b). At higher metallicity, the mean and dispersion of [α/Fe] rise, in stark contrast to the α/Fe trend in the Milky Way and that expected for other SF histories (e.g., Smecker-Hane et al. 2002). The increase in α/Fe with increasing metallicity is a clear signature for differential depletion (Prochaska & Wolfe 2002); i.e., large [α/Fe] ratios at high metallicity result from the greater adsorption of Fe onto dust grains.

Turning to the GRB DLAs, all of the [α/Fe] measurements are consistent with at least +0.5 dex, and the majority lie at greater than +0.6 dex. Two-sample survival analysis tests (e.g., Gehan) report a less than 0.1% probability that the [α/Fe] values of the QSO DLAs and GRB DLAs are drawn from the same parent population. We conclude that the GRB DLAs have systematically higher [α/Fe] ratios than the QSO DLAs. The question that follows is whether these higher values indicate enhanced α-abundances (nucleosynthesis) and/or a higher depletion level for Fe (dust).

From the nucleosynthetic viewpoint, one expects enhanced α/Fe in the gas near GRBs because (1) the progenitors are massive stars and (2) the high, specific SFRs of their host galaxies imply ages that are young compared to the timescales for Type Ia enrichment (Christensen et al. 2004). We contend that [α/Fe] $> +0.3$ dex is strongly expected for GRB DLA gas from nucleosynthesis enrichment alone (see also F. Calura et al. 2007, in preparation). Regarding dust, one may expect high depletion levels for gas in or near star-forming regions. This could also explain the offset in α/Fe between the GRB DLAs and QSO DLAs, especially if GRB DLAs have systematically higher metallicity (§ 3.2).

In § 3.3.2 we consider dust in greater depth. Before proceeding, we wish to emphasize the relatively low α/Fe value for GRB 050730: [α/Fe] $= 0.25 \pm 0.15$ at [α/H] $= -2.25$. If we were to

interpret this α/Fe ratio in terms of depletion, the intrinsic (nucleosynthetic) ratio would be approximately solar or even subsolar; this would require star formation with low efficiency over timescales of a few hundred Myr (Calura et al. 2003; Dessauges-Zavadsky et al. 2007). This mode of SF does not appear common for high-z GRB host galaxies (Christensen et al. 2004). In this one case, we argue that the gas is essentially undepleted. One may speculate further that the majority of QSO DLAs at low metallicity are also nearly undepleted and that their observed α/Fe ratios simply imply significant α-enrichment.

3.3.2. *Differential Depletion*

It is routine in QSO DLA studies to examine the Zn/Fe ratio to gauge the level of differential depletion (or Zn/Cr; Meyer & Roth 1990; Pettini et al. 1994). As discussed above, this assumes that the nucleosynthetic production of Zn tracks the Fe peak closely, such that enhancements in the gas-phase abundance of Zn/Fe are primarily due to Fe depletion. While this assumption should be questioned at the level of a few tenths dex (e.g., Prochaska et al. 2000), large Zn/Fe enhancements, especially at high metallicity, are unlikely to be explained by nucleosynthesis alone.

We present the Zn/Fe ratios of GRB DLAs and QSO DLAs in Figure 5*b*. Similar to the α/Fe ratios, the Zn/Fe values for the QSO DLAs increase with metallicity. Again, this is best explained by higher depletion levels at higher metallicity. The GRB DLAs do not exhibit this trend; the values are uniformly large. This suggests that the majority of GRB DLAs have large dust-to-metal ratios. Given the uncertainty on the nucleosynthesis of Zn, however, it is best to address this issue from yet another angle.

In Figure 5*c* we present upper limits to the Ti/Fe ratios of those GRB DLAs with observations of the Ti II λ1910 transitions. In stellar atmospheres, Ti behaves like an α-element (i.e., Ti tracks Si, O, and Mg in metal-poor stars; McWilliam 1997; Prochaska et al. 2000). In the Galactic ISM, Ti is highly refractory, and one generally observes $[\mathrm{Ti/Fe}]_{\mathrm{ISM}} < 0$ (Jenkins 1987). Therefore, Dessauges-Zavadsky et al. (2002) emphasized that observations of Ti/Fe lend to degenerate-free interpretation: supersolar Ti/Fe ratios indicate α-enhancement whereas subsolar Ti/Fe ratios require differential depletion. Therefore, the GRB DLAs with $[\mathrm{Ti/Fe}] \lesssim 0$ dex imply substantial depletion, especially in light of the large α/Fe ratios. We consider this definitive evidence that at least some GRB DLAs are highly depleted.

The results in Figures 5*b* and 5*c* argue that the GRB DLAs have at least modest depletion levels. We contend that differential depletion contributes at least +0.3 dex to [α/Fe] for most GRB DLAs; i.e., at least 50% or more of the Fe is locked into dust grains. It remains an open question, therefore, whether the intrinsic α/Fe ratios of GRB DLAs are enhanced relative to solar, as expected for young, star-forming regions (e.g., F. Calura et al. 2007, in preparation). While common practice is to examine the α/Zn ratio (again, using Zn as a proxy for Fe), these results are especially subject to the nucleosynthetic history of Zn. Nevertheless, examining α/Zn we find that the GRB DLAs primarily show lower limits that are consistent with the solar abundance but allow for large enhancements. In passing, we note that a large data set of α/Zn measurements for the GRB DLAs could inform the processes of Zn production and also interpretations of these measurements in QSO DLAs (Nissen et al. 2004).

3.3.3. N/α

Another abundance ratio of particular interest in terms of nucleosynthesis is N/α. Because N is believed to be produced primarily in the AGB phenomenon of intermediate-mass stars (e.g., Meynet & Maeder 2002), the N/α ratio provides a diagnostic of the SF history of the galaxy, especially at early times (Henry et al. 2000). Atomic nitrogen is the dominant ionization state in neutral regions and, unfortunately, this low ion's transitions all lie within the Lyα forest. Therefore, the N abundance is difficult to measure in absorption-line systems: high-resolution data are required, and line-profile analysis is often required to recover N^0 column densities. Because N is nonrefractory, the observed ratios should nearly correspond to the intrinsic values. The only serious systematic uncertainties are ionization corrections (Prochaska et al. 2002a), which should be small for GRB DLAs given the very large H I column densities.

The current GRB DLA sample allows one to constrain the N^0 column density for only three GRB DLAs: GRB 050730, GRB 050820, and GRB 050922C. The N/α ratios are presented in Figure 5*d* in comparison with measurements made for the QSO DLAs (Prochaska et al. 2002a; Centurión et al. 2003; Dessauges-Zavadsky et al. 2006b). Although this is a small sample, it is evident that there is a large dispersion in [N/α] for the GRB DLAs. This indicates that their host galaxies have experienced a diverse range of SF histories.

Two of the N/α values (GRB 050820, GRB 050730) bracket the locus of observations for the QSO DLAs. These values are relatively high ($[\mathrm{N}/\alpha] \geq -1$), indicating a significant enhancement by intermediate-mass stars. This is not surprising for GRB 050820, in which the gas metallicity is large, implying several generations of SF. The N/α value for GRB 050730 (at metallicity $[\mathrm{M/H}] \approx -2$) suggests an age older than 200 Myr (Henry et al. 2000), which at $z = 4$ implies a formation redshift approaching the epoch of reionization.

The most intriguing measurement, however, is the upper limit to N/α in GRB 050922C. This limit lies well below even the so-called lower plateau of QSO DLA values (Prochaska et al. 2002a; Centurión et al. 2003). If this upper limit has a nucleosynthetic origin, it implies gas that has not been polluted by any intermediate-mass stars. Given this rather extreme value, it is important to further address ionization corrections; perhaps the low N/α value indicates an unusual ionization state for the gas (i.e., a high N^+/N^0 ratio). Because atomic nitrogen has a relatively large cross section to X-rays (Sofia & Jenkins 1998), it may be underabundant even in neutral regions. Both the GRB afterglow and the progenitor imply an enhanced radiation field, which could lead to high N^+/N^0 ratios. We are especially concerned about photoionization for GRB 050922C, given that it has a low Mg^0 column density and likely absorption by the N V doublet (Piranomonte et al. 2007). Equilibrium photoionization calculations, however, indicate that ionization corrections are generally less than 0.5 dex, even for an input spectrum as hard as a quasar (Prochaska et al. 2002b). In a future paper, we will perform a time-dependent calculation to track the effects of the afterglow on this and other ionization states relevant to our observations.

Unless the ionization corrections are larger than 0.5 dex, the limit on [N/α] lies below that of any other astrophysical environment. This is not especially surprising for a GRB event, however, especially one with very low metallicity. In this case, the galaxy may have initiated SF only very recently, and the observed metals may have no contribution from intermediate-mass stars. For a standard initial mass function, this requires an enrichment age of less than $\sim$30 Myr (Henry & Prochaska 2007). Future observations will reveal whether low N/α values are characteristic of a larger sample of GRB DLAs.

3.4. *Atomic Carbon*

In the Galaxy, an excellent tracer of cold, dense gas is atomic carbon. Because C^0 has an ionization potential below 1 ryd, it is

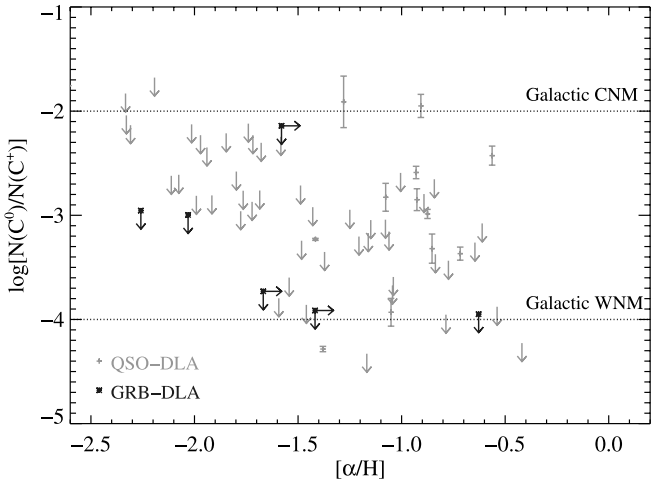

FIG. 6.—C^0/C^+ ratios of the GRB DLAs (*black*) and QSO DLAs (*gray*) inferred from column density measurements of C I transitions and by assuming $\log N(C^+) = [\alpha/H] + \log N_{H\,I} - 4$. Typical values of the cold neutral medium of the Galactic ISM are $C^0/C^+ = 10^{-2}$ (Jenkins & Shaya 1979), while significantly lower values (10^{-4}) correspond to the warm neutral medium (Liszt 2002). We interpret the observations as more reflective of the latter phase of the ISM, but caution that the results are sensitive to the far-UV intensity, metallicity, and cosmic-ray flux through the gas. [*See the electronic edition of the Journal for a color version of this figure.*]

generally photoionized by the ambient far-UV radiation field of the ISM. In cold and dense regions, however, the recombination rate (proportional to the electron and carbon densities) is sufficiently large that cold clouds frequently show detectable absorption from C I transitions (e.g., Jenkins & Tripp 2001). For standard Galactic ISM conditions, the C^0/C^+ ratio is $\approx 10^{-2}$ in the cold neutral medium and decreases to $\approx 10^{-4}$ in the warm neutral medium (Liszt 2002). These ratios, of course, are sensitive to the gas metallicity, far-UV radiation field, and cosmic-ray flux of the ISM (Liszt 2002; Wolfe et al. 2003). Nevertheless, very low C^0/C^+ values generally imply gas with density less than 10 particles per cm^3.

Figure 6 presents the C^0/C^+ ratios estimated for the GRB DLAs and QSO DLAs (sample HR-A). While we can measure $N(C^0)$ directly from C I transitions, the C II transitions are generally too saturated to provide even a valuable lower limit to $N(C^+)$. Therefore, we infer $N(C^+)$ from the $[\alpha/H]$ abundance and $N_{H\,I}$ value, assuming $[\alpha/C] = +0.3$ (i.e., a modest α-enhancement; Akerman et al. 2004):

$$\log N(C^+) = [\alpha/H] + \log N_{H\,I} - 12 + 8.3. \quad (2)$$

Note that this calculation is actually independent of the $N_{H\,I}$ value. None of the GRB DLAs in our sample have a positive detection, although Vreeswijk et al. (2007) reported the detection of C I in GRB DLA 060418, with a value consistent with our upper limit. Because the metal-line column densities of the GRB DLAs are large, the upper limits to C^0/C^+ generally lie below those of the QSO DLAs even though the latter are derived from higher S/N data. The observations suggest that the gas in GRB DLAs (and many QSO DLAs) is dominated by a warm, less dense phase. We caution again, however, that the predicted C^0/C^+ values are sensitive to the far-UV flux, which is likely to be enhanced near the GRB. A more cautious interpretation of the data is that it offers additional yet nonconclusive support that GRB DLA gas is not characteristic of the Galactic cold neutral medium.

4. DISCUSSION

4.1. *General Characteristics of the ISM near Star-forming Regions*

Reviewing the results presented in § 3, we summarize the properties of gas observed surrounding GRB afterglows as having:

1. Very large H I column densities with median $N_{H\,I} \approx 10^{21.6}$ cm^{-2}.
2. A wide range of metallicities (1/100 to nearly solar) with median larger than 1/10 solar.
3. Observed α/Fe ratios in excess of 3 times the solar abundance, reflecting enrichment by massive stars (Type II SNe) and/or differential depletion.
4. Large [Zn/Fe] values and several solar or subsolar [Ti/Fe] upper limits that indicate substantial differential depletion.
5. A dispersion of $[N/\alpha]$, indicating a diverse set of SF histories. We identify one case (GRB 050922C) with an extremely low value, suggesting gas enriched solely by massive stars.

At first glance, the observation of large H I surface densities and significantly depleted, chemically enriched gas appears to reflect the conditions expected for actively star-forming regions (i.e., molecular clouds). Quantitatively, however, we find that the GRB DLA properties are more characteristic of the ambient ISM of modern galaxies. As several authors have noted for individual GRB DLAs (Savaglio & Fall 2004; Penprase et al. 2006; Shin et al. 2006), the observed depletion levels are more representative of warm (i.e., less dense) clouds in the Galactic ISM (see also Savaglio 2006). On the other hand, the majority of GRB DLAs have subsolar metallicity, and a direct comparison with the Galactic ISM may not be appropriate. Unfortunately, the differential depletion characteristics of cold, dense gas in other galaxies (e.g., the Magellanic Clouds) have not been extensively measured, in part because dust obscuration challenges the analysis. In the Small Magellanic Cloud (SMC), one does observe highly depleted gas along the sight line to Sk 155, but one also finds modest depletions in clouds where C I analysis indicates a large density (>100 cm^{-3}; Welty et al. 2001, 2006; Sofia et al. 2006). We cautiously conclude that the depletion levels observed for the GRB DLAs are generally lower than that observed for cold, dense clouds in the local universe. It would be very valuable to independently estimate the density of gas responsible for GRB DLAs.

Throughout this paper, we have presented additional observations that argue that the GRB DLAs do not arise in a cold, dense phase. First, the gas has a very low molecular fraction (Vreeswijk et al. 2004; Tumlinson et al. 2007). Although a low molecular fraction could result from photoionization by the progenitor, nearby O and B stars, and the GRB afterglow, we have argued that the gas lies at $\gtrsim$100 pc from the GRB, where these effects may be lessened. If the gas has a large particle density ($n_H > 10^3$ cm^{-3}), then it would be difficult to maintain such a low H_2 fraction (Tumlinson et al. 2007).

Second, the only atomic line routinely measured in the GRB DLAs is Mg I, and its large dielectronic recombination coefficient does not require cold, dense gas. In § 3.4 we presented upper limits on C^0/C^+, which argue against gas with characteristics like the dense CNM of the Milky Way. Third, there are no especially anomalous abundance patterns observed for the gas (e.g., extreme metallicity, very high α/Fe ratios), which could occur if the gas represented partially mixed SN ejecta or circumstellar material. Altogether, we conclude that the gas revealed by GRB afterglow spectra represents the ISM near the GRB but not gas directly associated with its own molecular cloud.

4.2. *Comparisons with QSO DLAs*

In § 4.1 we argued that the GRB DLAs represent gas from the ambient ISM of their host galaxies. The large $N_{\rm H\,I}$ values of QSO DLAs argue that these sight lines also penetrate the ISM of high-z galaxies. Furthermore, the majority of QSO DLAs have depletion patterns, low C^+0/C^+ ratios, and low molecular fractions that are not characteristic of cold, dense gas in the Galaxy. In this respect, it is fair to compare the observations of the two populations to address whether they are drawn from the same parent population of galaxies. In § 3 we compared the $N_{\rm H\,I}$ values, metallicity, and relative abundance ratios of the QSO DLAs and GRB DLAs. The latter are characterized by higher $N_{\rm H\,I}$ values, higher α/Fe and Zn/Fe ratios, and higher metallicities. These differences beg the following question. *Are GRB DLAs and QSO DLAs drawn from distinct distributions of host galaxies*?

We contend that the observations presented in this paper do not contradict the null hypothesis that GRB DLAs and QSO DLAs have identical parent populations of galaxies, but their differences can be explained by sight lines with distinct impact parameter distributions. Although offsets exist in [M/H] and the X/Fe ratios, the differences are relatively small (<0.5 dex). Typical observed gradients in the metallicity of stars and H II regions of local galaxies imply a variation of at least 0.3 dex from the center of the galaxy to the radii roughly corresponding to $N_{\rm H\,I} = 2 \times 10^{20}$ cm^{-2} (e.g., Kennicutt et al. 2003; Chen et al. 2005; Luck et al. 2006). Furthermore, the H I surface density and volume density are undoubtedly larger toward the center of the galaxy (at least until the gas becomes molecular). And it is reasonable to expect that higher-metallicity, denser gas will exhibit larger depletion levels than more tenuous gas at the outer edges of H I disks.

At present, the only distribution with an especially large offset (>1 dex difference in median value) is the $N_{\rm H\,I}$ values. While differences in the impact parameters of GRB DLAs and QSO DLAs may explain the offsets in the median of the distributions for $N_{\rm H\,I}$, [M/H], and X/Fe ratios, the identification of many GRB DLAs with $N_{\rm H\,I} > 10^{22}$ cm^{-2} and *none* in the QSO DLA sample is striking. In § 3.1 we demonstrated that the GRB DLA $N_{\rm H\,I}$ distribution is reasonably well explained by an H II region embedded with an exponential H I disk with central column density $\log N_0 = 10^{22}$ cm^{-2}. While this simplistic model is a good description of the observations, it does lead to a conflict with the H I frequency distribution $f(N_{\rm H\,I})$ observed for the QSO DLAs. If the majority of high-z galaxies have $\log N_0 = 10^{22}$ cm^{-2}, then one would not observe a break in $f(N_{\rm H\,I})$ at $N_{\rm H\,I} \approx 10^{21.5}$ cm^{-2} as observed (Prochaska et al. 2005). One possible resolution for this conflict is that GRB DLA sight lines are obscured by dust from magnitude-limited QSO surveys. Let us now consider this hypothesis in greater detail.

4.3. *Can QSO DLA Samples Probe GRB DLA Sight Lines?*

As Figure 2 reveals, a significant fraction of GRB DLAs have $N_{\rm H\,I} \geq 10^{22}$ cm^{-2}, yet not one of the ≈500 QSO DLAs discovered thus far has $N_{\rm H\,I} > 10^{21.9}$ cm^{-2}. An analysis of the SDSS data set actually requires that the QSO DLAs exhibit a break in their H I frequency distribution $f(N_{\rm H\,I})$ at $N_{\rm H\,I} \approx 10^{21.5}$ cm^{-2} to explain the absence of large $N_{\rm H\,I}$ absorbers (Prochaska et al. 2005). This is most easily seen by extrapolating the $f(N_{\rm H\,I}) \propto N_{\rm H\,I}^{-2}$ power law observed at $N_{\rm H\,I} < 1021$ cm^{-2} to larger column densities. One predicts that there should be ≈10 DLAs with $N_{\rm H\,I} \geq 10^{22}$ cm^{-2} per 500 observed. The absence of a single QSO DLA with this column density indicates that $f(N_{\rm H\,I})$ has a steeper than $N_{\rm H\,I}^{-2}$ dependence at these column densities. The observation of a break in $f(N_{\rm H\,I})$ and the routine observation of $N_{\rm H\,I} > 1022$ cm^{-2} in GRB DLAs raises concerns that dust obscuration is biasing the QSO DLA sample against large $N_{\rm H\,I}$ values.

There is additional (circumstantial) evidence for a dust obscuration bias in QSO DLAs. First, QSO DLAs with a combination of large $N_{\rm H\,I}$ and high metallicity (metal-strong DLAs), i.e., potentially large dust columns, are rare (Boisse et al. 1998; Herbert-Fort et al. 2006). Second, every DLA is enriched by heavy metals with metallicity [M/H] > −3 (Prochaska et al. 2003a), and many have relative abundance ratios (e.g., Zn/Fe) indicative of differential dust depletion (Pettini et al. 1994; Prochaska & Wolfe 2002). Third, several quasars with intervening DLAs show significant reddening that can be attributed to the absorber (Vladilo et al. 2006), although the average reddening is likely to be small (Murphy & Liske 2004). Motivated by these observations, we test whether QSO DLA samples would be likely to include GRB DLA sight lines if background quasars were placed directly on the sight line.

We begin by deriving the dust-to-gas ratios of the GRB DLAs. In the following, we assume that the GRB DLA dust properties are best matched by those observed for the SMC. We make this choice because (1) no GRB DLA to date has exhibited the 2175 Å dust feature characteristic of the Milky Way and Large Magellanic Cloud (LMC) extinction laws (e.g., Mirabal et al. 2002; Savaglio & Fall 2004; Ellison et al. 2006); and (2) the metallicities of GRB DLAs are representative of the SMC. We derive the dust-to-gas ratio of the DLAs relative to the SMC: $\kappa/\kappa_{\rm SMC}$ by assuming that the SMC has metallicity $[{\rm M/H}]_{\rm SMC} = -0.7$ and that 90% of its refractory elements are depleted from the gas phase, i.e., $[{\rm M/Fe}]_{\rm SMC} = +1$ (Welty et al. 1997, 2001). In this case, the relative dust-to-gas ratio is

$$\frac{\kappa}{\kappa_{\rm SMC}} = 10^{[{\rm M/H}]+0.7}\left[\frac{1-10^{(\Delta_i-[{\rm M/Fe}])}}{1-10^{-1}}\right], \qquad (3)$$

where Δ_i allows for a nucleosynthetic contribution to the observed [M/Fe] value, and we assume $\Delta_i = 0$ for the SMC. For the GRB DLAs, we adopt the [M/H] and [M/Fe] values listed in Table 3. In the majority of cases, M is sulfur and the remainder assume Zn or Si. In the following, we will assume $\Delta_i = 0.3$ dex for the GRB DLAs and 0.2 dex for the QSO DLAs. The high specific SFRs observed for GRB host galaxies indicate young ages and, therefore, gas enriched by massive stars giving α-enriched abundances ($[\alpha/{\rm Fe}] > +0.2$). Similarly, the QSO DLAs show a plateau of $[{\rm Si/Fe}] = +0.25$ dex values at low metallicity, indicative of Type II enrichment (Prochaska & Wolfe 2002), and enhanced α/Fe ratios in "dust free" systems (Dessauges-Zavadsky et al. 2006b). In any case, the results are not sensitive to our choices for Δ_i unless we allow $\Delta_i > 0.5$ dex for the GRB DLAs or $\Delta_i > 0.3$ dex for the QSO DLAs.

Figure 7 shows the $\kappa/\kappa_{\rm SMC}$ values for the GRB DLAs and also the echelle sample (HR-E) of QSO DLAs. Both samples exhibit a wide range of dust-to-gas ratios relative to the SMC. We also find that the GRB DLAs show a higher fraction of large values ($\kappa/\kappa_{\rm SMC} \gtrsim 1$). Using the observed $N_{\rm H\,I}$ values and assuming SMC dust properties, we can convert these dust-to-gas ratios into visual extinction, A_V. Specifically, we adopt two empirical relations: (1) the observed reddening in the SMC (Tumlinson et al. 2002),

$$\log E(B-V) = \log N_{\rm H\,I} - 22.95, \qquad (4)$$

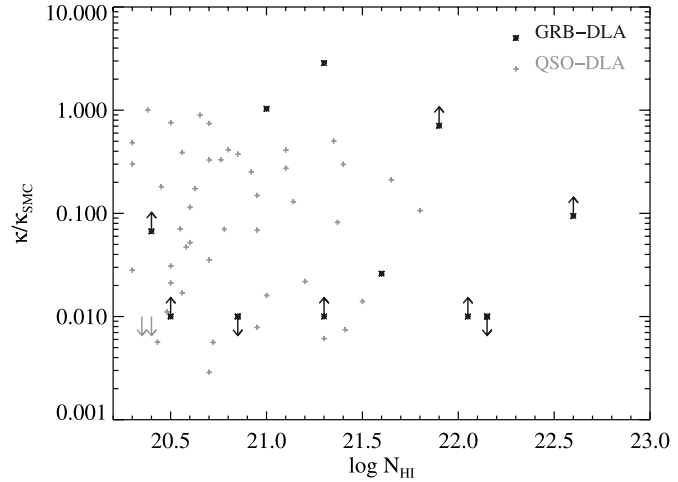

FIG. 7.—Dust-to-gas ratio κ of the GRB DLAs (*black*) and QSO DLAs (*gray*) relative to the dust-to-gas ratio of the SMC ($\kappa_{\rm SMC}$) as a function of the H I column density. [*See the electronic edition of the Journal for a color version of this figure.*]

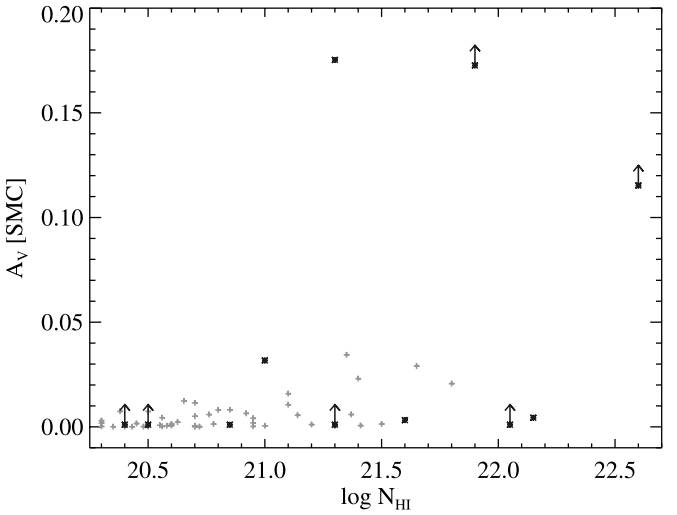

FIG. 8.—Predicted visual extinctions A_V for the GRB DLA and QSO DLA sight lines, assuming the dust-to-gas ratios presented in Fig. 7 and assuming the dust properties of the SMC (Tumlinson et al. 2002; Gordon et al. 2003). All of the QSO DLA sight lines show very small values ($A_V < 0.05$ mag). In contrast, the GRB DLAs show a nearly bimodal population with several small values and several sight lines approaching 0.2 mag. Note that $A_V = 0.1$ mag corresponds to an extinction of 0.6 mag, assuming the SMC extinction law. [*See the electronic edition of the Journal for a color version of this figure.*]

and (2) a linear relation between A_V and $E(B-V)$ (Gordon et al. 2003) modified by the dust-to-gas ratio

$$A_V = 2.74[E(B-V)]\frac{\kappa}{\kappa_{\rm SMC}}. \quad (5)$$

Figure 8 presents the A_V values against the H I column density for the GRB DLAs compared against QSO DLAs. All of the QSO DLAs have $A_V < 0.05$ mag (see also Prochaska & Wolfe 2002). It is not surprising, therefore, that one observes very little reddening of quasar spectra by QSO DLAs (Murphy & Liske 2004). In contrast, the estimated A_V values for approximately half the GRB DLAs are substantially larger than the QSO DLA distribution ($A_V > 0.1$ mag). At $A_V = 0.1$ mag, the extinction at the Lyα transition is $A_{{\rm Ly}\alpha} = 0.6$ mag, assuming the SMC extinction law (Prevot et al. 1984). This is a considerable but not overwhelming level of extinction. It is interesting to note that there is no obvious correlation between A_V and $N_{\rm H\,I}$, at least for A_V values greater than 0.05 mag. We also note that the A_V values presented in Figure 8 are roughly consistent with the A_V values inferred from broadband photometry or spectrophotometry of GRB afterglows (e.g., Mirabal et al. 2002; Vreeswijk et al. 2004; Savaglio & Fall 2004; Butler et al. 2006). On the other hand, our A_V values appear to be at odds with those inferred from X-ray absorption measurements (e.g., Watson et al. 2006; Butler et al. 2006), which has led some authors to invoke "gray" extinction laws for the dust-enveloping GRBs (Galama & Wijers 2001). This issue will be addressed in greater detail in a future paper.

Finally, we examine whether the inferred A_V values for the GRB DLA sight lines are sufficiently large to bias against their detection in QSO samples. To estimate the effects, we assessed the S/N at the center of the Lyα profile of each QSO DLA in the SDSS DR3 sample. Specifically, we measured the median S/N using the continuum adopted in the fits to the Lyα profiles by Prochaska et al. (2005). By the definition of their statistical sample, the S/N exceeds 4 pixel^{-1} in each case. We then lowered the S/N by adopting an extinction, A_V, assuming that the noise is quasar-dominated,

$$\mathrm{S/N} = \frac{(\mathrm{S/N})_0}{\sqrt{10^{A_{{\rm Ly}\alpha}/2.5}}}. \quad (6)$$

The fraction of QSO DLAs that satisfy the S/N > 4 pixel^{-1} criterion is shown in Figure 9 as a function of A_V. For $A_V < 0.2$ mag, dust obscuration has a relatively small impact on the QSO DLA sample. We cautiously conclude, therefore, that the majority of observed GRB DLAs would also be observed along quasar sight lines.

This conclusion, however, is subject to a few caveats. First, the exercise described by Figure 9 does not account for quasars that would become too red or too faint to satisfy the QSO target criteria for the SDSS (Richards et al. 2004). We suspect, however, that this effect is much smaller than the S/N cut we have applied (M. Murphy et al. 2007, in preparation). Second, several of the $\kappa/\kappa_{\rm SMC}$ values for the GRB DLAs are lower limits because of line saturation. It is possible that these have $A_V > 0.4$ mag and

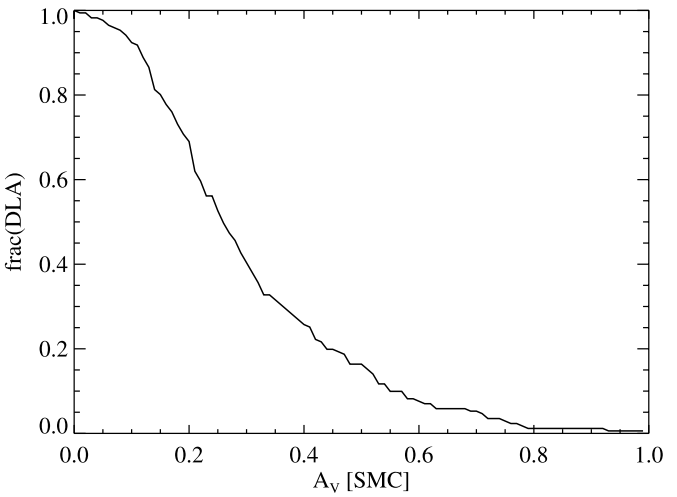

FIG. 9.—Fraction of DLAs recovered from the SDSS QSO DLA survey of Prochaska et al. (2005) as a function of additional visual extinction (A_V) for the DLAs. For $A_V < 0.2$ mag, the effect of obscuration is mild, while only a small fraction of QSO DLAs with $A_V > 0.4$ mag would be recovered in the SDSS survey.

would have a small probability of entering the QSO DLA sample. Third, all of the results assume SMC extinction. This assumption has two implications: (1) it establishes the reddening per H I atom (scaled by metallicity; eq. [4]) and (2) the shape of the extinction law that determines $A_{\rm Ly\alpha}/A_V$. Regarding the latter aspect, the SMC has the steepest extinction law of local galaxies. Other ("grayer") dust laws would generally lead to less extinction at Lyα. The reddening per H I atom in the SMC, however, is smaller than the Milky Way and not only because of the SMC's lower metallicity (Welty et al. 2006). Fourth, we have ignored the possibility that a significant column of dust exists in the H II region surrounding the GRB. This could be revealed by broadband photometry of the afterglow compared against A_V estimations from the observed metal column densities. Finally, we note that a non-negligible fraction of GRB afterglows are severely reddened, most likely by dust surrounding the event (Levan et al. 2006; Pellizza et al. 2006). These "dark bursts" do not enter our GRB DLA sample and likely have A_V values much larger than those presented in Figure 8. At present, this extremely dusty gas is not well probed by GRB or QSO observations.

These concerns aside, our analysis suggests that many (if not all) of the GRB DLAs in our sample could be detected in modern QSO DLA surveys. If confirmed by larger samples, then the very low incidence of QSO DLAs with $N_{\rm H\,I} \geq 10^{22}$ cm^{-2} must be explained by a substantial decrease in the cross section of gas with these column densities. To avoid conflict with the observed $f(N_{\rm H\,I})$ distribution, one requires that the cross section of the regions probed by GRB DLAs must be less than 1% of the cross section corresponding to the damped Lyα criterion, $\log N_{\rm H\,I} = 20.3$. Characterizing the latter by a radius $r_{20.3}$, we require $r_{\rm GRB} < r_{20.3}/10$. This relation is rather easily achieved if $r_{\rm GRB}$ is 100 pc or less, but could pose a problem if $r_{\rm GRB} \gtrsim 1$ kpc (Vreeswijk et al. 2007).

We wish to thank Arthur M. Wolfe for helpful discussions and for allowing us to analyze results on QSO DLAs prior to the public release of these data. We thank E. Ramirez-Ruiz for constructive comments on an early version of this manuscript and J. Fynbo for detailed comments on the submitted version. J. X. P. is partially supported by NASA/*Swift* grant NNG 05-GF55G and an NSF CAREER grant (AST 05-48180).

Facilities: Keck:I (LRIS, ESI, HIRES), Keck:II (LRIS, ESI, HIRES), VLT:Antu (FORS2, UVES), VLT:Kueyen (FORS2, UVES), VLT:Melipal (FORS2, UVES), VLT:Yepun (FORS2, UVES), ING:Herschel (ISIS), Magellan:Baade (MIKE), Magellan:Clay (MIKE), Subaru (FOCAS)

REFERENCES

Akerman, C. J., et al. 2004, A&A, 414, 931
Barth, A. J., et al. 2003, ApJ, 584, L47
Berger, E., et al. 2006, ApJ, 642, 979
Blitz, L. 1993, in Protostars and Planets III, ed. E. H. Levy & J. I. Lunine (Tucson: Univ. Arizona Press), 125
Blitz, L., et al. 2007, in Protostars and Planets V, ed. B. Reipurth, D. Jewitt, & K. Keil (Tucson: Univ. Arizona Press), 81
Bloom, J. S., Kulkarni, S. R., & Djorgovski, S. G. 2002, AJ, 123, 1111
Boisse, P., et al. 1998, A&A, 333, 841
Butler, N. R., et al. 2006, ApJ, 652, 1390
Calura, F., Matteucci, F., & Vladilo, G. 2003, MNRAS, 340, 59
Castro, S., et al. 2003, ApJ, 586, 128
Centurión, M., et al. 2003, A&A, 403, 55
Chen, H.-W., Kennicutt, R. C., Jr., & Rauch, M. 2005, ApJ, 620, 703
Chen, H.-W., et al. 2005, ApJ, 634, L25
———. 2007, ApJ, 663, 420
Christensen, L., Hjorth, J., & Gorosabel, J. 2004, A&A, 425, 913
Dekker, H., et al. 2000, Proc. SPIE, 4008, 534
Dessauges-Zavadsky, M., Prochaska, J. X., & D'Odorico, S. 2002, A&A, 391, 801
Dessauges-Zavadsky, M., et al. 2001, A&A, 370, 426
———. 2006a, ApJ, 648, L89
———. 2006b, A&A, 445, 93
———. 2007, A&A, 470, 431
Draine, B. T., & Hao, L. 2002, ApJ, 569, 780
Ellison, S. L., et al. 2006, MNRAS, 372, L38
Fall, S. M., & Pei, Y. C. 1993, ApJ, 402, 479
Feigelson, E. D., & Nelson, P. I. 1985, ApJ, 293, 192
Fenner, Y., Prochaska, J. X., & Gibson, B. K. 2004, ApJ, 606, 116
Fiore, F., et al. 2005, ApJ, 624, 853
Fruchter, A., Krolik, J. H., & Rhoads, J. E. 2001, ApJ, 563, 597
Fruchter, A. S., et al. 2006, Nature, 441, 463
Fynbo, J. P. U., et al. 2002, in Lighthouses of the Universe, ed. M. Gilfanov, R. Sunyaev, & E. Churazov (Berlin: Springer), 187
———. 2006a, A&A, 451, L47
———. 2006b, Nature, 444, 1047
Galama, T. J., & Wijers, R. A. M. J. 2001, ApJ, 549, L209
Gehrels, N. A. 2000, Proc. SPIE, 4140, 42
Gordon, K. D., et al. 2003, ApJ, 594, 279
Guetta, D., & Piran, T. 2007, J. Cosmol. Astropart. Phys., 7, 3
Hammer, F., et al. 2006, A&A, 454, 103
Henry, D., & Prochaska, J. 2007, PASP, submitted
Henry, R. B. C., Edmunds, M. G., & Köppen, J. 2000, ApJ, 541, 660
Herbert-Fort, S., et al. 2006, PASP, 118, 1077
Hjorth, J., et al. 2003, Nature, 423, 847
Hoffman, R. D., et al. 1996, ApJ, 460, 478
Howk, J. C., & Sembach, K. R. 1999, ApJ, 523, L141
Jakobsson, P., et al. 2006a, A&A, 447, 897
———. 2006b, A&A, 460, L13
Jenkins, E. B. 1986, ApJ, 304, 739
———. 1987, in Interstellar Processes, ed. D. J. Hollenbach & H. A. Thronson, Jr. (Dordrecht: Reidel), 533
Jenkins, E. B., & Shaya, E. J. 1979, ApJ, 231, 55
Jenkins, E. B., & Tripp, T. M. 2001, ApJS, 137, 297
Jensen, B. L., et al. 2001, A&A, 370, 909
Kann, D. A., Klose, S., & Zeh, A. 2006, ApJ, 641, 993
Kawai, N., et al. 2006, Nature, 440, 184
Kennicutt, R. C., Jr., Bresolin, F., & Garnett, D. R. 2003, ApJ, 591, 801
Kewley, L. J., et al. 2007, AJ, 133, 882
Kobulnicky, H. A., & Kewley, L. J. 2004, ApJ, 617, 240
Langer, N., & Norman, C. A. 2006, ApJ, 638, L63
Lanzetta, K. M. 1993, in The Environment and Evolution of Galaxies, ed. J. M. Shull & H. A. Thronson (Dordrecht: Kluwer), 237
Ledoux, C., Petitjean, P., & Srianand, R. 2003, MNRAS, 346, 209
Ledoux, C., et al. 2006, A&A, 457, 71
Le Floc'h, E., et al. 2003, A&A, 400, 499
Levan, A., et al. 2006, ApJ, 647, 471
Liszt, H. 2002, A&A, 389, 393
Lu, L., et al. 1996, ApJS, 107, 475
Luck, R. E., Kovtyukh, V. V., & Andrievsky, S. M. 2006, AJ, 132, 902
McWilliam, A. 1997, ARA&A, 35, 503
Metzger, M. R., et al. 1997, Nature, 387, 878
Meyer, D. M., & Roth, K. C. 1990, ApJ, 363, 57
Meynet, G., & Maeder, A. 2002, A&A, 381, L25
Mirabal, N., et al. 2002, ApJ, 578, 818
———. 2006, ApJ, 643, L99
Mo, H. J., Mao, S., & White, S. D. M. 1998, MNRAS, 295, 319
Modjaz, M., et al. 2007, AJ, submitted (astro-ph/0701246)
Molaro, P., et al. 2001, ApJ, 549, 90
Möller, P., Fynbo, J. P. U., & Fall, S. M. 2004, A&A, 422, L33
Möller, P., et al. 2002, ApJ, 574, 51
Murphy, M. T., & Liske, J. 2004, MNRAS, 354, L31
Nissen, P. E., et al. 2004, A&A, 415, 993
Pellizza, L. J., et al. 2006, A&A, 459, L5
Penprase, B. E., et al. 2006, ApJ, 646, 358
Perna, R., & Lazzati, D. 2002, ApJ, 580, 261
Pettini, M., Boksenberg, A., & Hunstead, R. W. 1990, ApJ, 348, 48
Pettini, M., et al. 1994, ApJ, 426, 79
Piranomonte, S., et al. 2007, A&A, submitted
Prevot, M. L., et al. 1984, A&A, 132, 389
Prochaska, J. X. 2006, ApJ, 650, 272
Prochaska, J. X., Chen, H.-W., & Bloom, J. S. 2006, ApJ, 648, 95

Prochaska, J. X., & Herbert-Fort, S. 2004, PASP, 116, 622
Prochaska, J. X., Herbert-Fort, S., & Wolfe, A. M. 2005, ApJ, 635, 123
Prochaska, J. X., & Wolfe, A. M. 1999, ApJS, 121, 369
———. 2002, ApJ, 566, 68
Prochaska, J. X., et al. 2000, AJ, 120, 2513
———. 2001, ApJS, 137, 21
———. 2002a, PASP, 114, 933
———. 2002b, ApJ, 571, 693
———. 2003a, ApJ, 595, L9
———. 2003b, ApJS, 147, 227
———. 2004, ApJ, 611, 200
———. 2005, GCN Circ. 3971, http://gcn.gsfc.nasa.gov/gcn/gcn3/3971.gcn3
———. 2007a, ApJS, 168, 231
———. 2007b, ApJS, 171, 29
———. 2007c, ApJ, submitted (astro-ph/0703701)
Prochter, G. E., et al. 2006, ApJ, 648, L93
Qian, Y.-Z., & Wasserburg, G. J. 2003, ApJ, 596, L9
Ramirez-Ruiz, E., Trentham, N., & Blain, A. W. 2002, MNRAS, 329, 465
Razoumov, A. O., et al. 2006, ApJ, 645, 55
Reichart, D. E., & Price, P. A. 2002, ApJ, 565, 174
Richards, G. T., et al. 2004, ApJS, 155, 257
Savaglio, S. 2006, New J. Phys., 8, 195
Savaglio, S., & Fall, S. M. 2004, ApJ, 614, 293
Savaglio, S., Fall, S. M., & Fiore, F. 2003, ApJ, 585, 638
Sheinis, A. I., et al. 2000, Proc. SPIE, 4008, 522
Shin, M.-S., et al. 2006, ApJ, submitted (astro-ph/0608327)
Smecker-Hane, T. A., et al. 2002, ApJ, 566, 239
Sneden, C., Gratton, R. G., & Crocker, D. A. 1991, A&A, 246, 354
Sofia, U. J., & Jenkins, E. B. 1998, ApJ, 499, 951
Sofia, U. J., et al. 2006, ApJ, 636, 753
Sollerman, J., et al. 2005, NewA, 11, 103
Solomon, P. M., & Rivolo, A. R. 1989, ApJ, 339, 919
Spergel, D. N., et al. 2007, ApJS, 170, 377
Stanek, K. Z., et al. 2003, ApJ, 591, L17
———. 2006, Acta Astron., 56, 333
Tinsley, B. M. 1979, ApJ, 229, 1046
Totani, T. 1999, ApJ, 511, 41
Tumlinson, J., et al. 2002, ApJ, 566, 857
———. 2007, ApJ, in press (astro-ph/0703666)
Vink, J. S., & de Koter, A. 2005, A&A, 442, 587
Vladilo, G., et al. 2006, A&A, 454, 151
Vogt, S. S., et al. 1994, Proc. SPIE, 2198, 362
Vreeswijk, P. M., et al. 2004, A&A, 419, 927
———. 2006, A&A, 447, 145
———. 2007, A&A, 468, 83
Wasserburg, G. J., & Qian, Y.-Z. 2000, ApJ, 538, L99
Watson, D., et al. 2006, ApJ, 652, 1011
Waxman, E., & Draine, B. T. 2000, ApJ, 537, 796
Welty, D. E., et al. 1997, ApJ, 489, 672
———. 2001, ApJ, 554, L75
———. 2006, ApJS, 165, 138
White, G. J., et al. 1999, A&A, 342, 233
Wijers, R. A. M. J., et al. 1998, MNRAS, 294, L13
Wolf, C., & Podsiadlowski, P. 2007, MNRAS, 375, 1049
Wolfe, A. M., Gawiser, E., & Prochaska, J. X. 2005, ARA&A, 43, 861
Wolfe, A. M., Prochaska, J. X., & Gawiser, E. 2003, ApJ, 593, 215
Wolfe, A. M., et al. 1986, ApJS, 61, 249
Woosley, S. E. 1993, ApJ, 405, 273
Woosley, S. E., & Bloom, J. S. 2006, ARA&A, 44, 507
Woosley, S. E., & Heger, A. 2006, ApJ, 637, 914
Woosley, S. E., & Weaver, T. A. 1995, ApJS, 101, 181
Zwaan, M. A., & Prochaska, J. X. 2006, ApJ, 643, 675